Cell Tissue Res (2014) 356:405–416
DOI 10.1007/s00441-014-1802-3

REGULAR ARTICLE

Cloning of *PaAtg8* and roles of autophagy in adaptation to starvation with respect to the fat body and midgut of the Americana cockroach, *Periplaneta americana*

Moon Soo Park · Makio Takeda

Received: 9 October 2013 / Accepted: 31 December 2013 / Published online: 4 April 2014

Abstract Starvation, in particular amino acid deprivation, induces autophagy in trophocytes (adipocytes), the major component of the fat body cell types, in the larvae of *Drosophila melanogaster*. However, the fat body of cockroach has two additional cell types: urocytes depositing uric acid in urate vacuoles as a nitrogen resource and mycetocytes harboring an endosymbiont, *Blattabacterium cuenoti*, which can synthesize amino acids from the metabolites of the stored uric acid. These cells might complement the roles of autophagy in recycling amino acids in the fat body or other organs of cockroaches under starvation. We investigate the presence of autophagy in tissues such as the fat body and midgut of the American cockroach, *Periplaneta americana*, under starvation by immunoblotting with antibody against Atg8, a ubiquitin-like protein required for the formation of autophagosomes and by electron microscopy. Corresponding changes in acid phosphatase activity were also investigated as representing lysosome activity. Starvation increased the level of an autophagic marker, Atg8-II, in both the tissues, extensively stimulating the formation of autophagic compartments in trophocytes of the fat body and columnar cells of the midgut for over 2 weeks. Acid phosphatase showed no significant increase in the fat body of the starved cockroaches but was higher in the midgut of the continuously fed animals. Thus, a distinct autophagic mechanism operates in these tissues under starvation of 2 weeks and longer. The late induction of autophagy implies exhaustion of the stored uric acid in the fat body. High activity of acid phosphatase in the midgut of the fed cockroaches might represent enhanced assimilation and not an autophagy-related function.

Keywords Autophagy · Bacteriocyte · Lysosome · Starvation · Urocyte · *Periplaneta americana*

M. S. Park
Research Center for Environmental Genomics, Kobe University, 1-1 Rokkodai-cho, Nada-ku, Kobe 657-8501, Japan

M. Takeda (✉)
Insect Science Laboratory, Graduate School of Agricultural Science, Kobe University, 1-1 Rokkodai-cho, Nada-ku, Kobe 657-8501, Japan
e-mail: mtakeda@kobe-u.ac.jp

Introduction

Autophagy, a cellular self-digestion system, is conserved among various eukaryotes such as yeast, nematodes, plants, vertebrates and invertebrates (Kovács et al. 1981; Schworer et al. 1981; Tsukada and Ohsumi 1993; Hanaoka et al. 2002; Meléndez et al. 2003; Mizushima et al. 2004; Rusten et al. 2004; Scott et al. 2004; Barth et al. 2011; Rost-Roszkowska et al. 2012). Double-membrane vesicles are initially formed that enclose cytoplasmic components. The enclosed structures are called autophagosomes and require Atg8-II, which is cleaved Atg8 (Atg8-I), tethered to phosphatidylethanolamine (PE) at the C-terminal (Kirisako et al. 1999; Kabeya et al. 2000; Amar et al. 2006; Nakatogawa et al. 2007). Autolysosomes, which are autophagosomes fused with lysosomes for the degradation of the enclosed components, transport recycled amino acids into the cytoplasm through the membrane (Mizushima et al. 2008; He and Klionsky 2009).

Autophagy is induced under starvation in various tissues of mice, such as liver, muscle tissues and pancreas (Mizushima et al. 2004). In larvae of *Drosophila melanogaster*, autophagy is observed in adipocytes of the fat body, the mammalian counterpart of which is the liver (Rusten et al. 2004; Scott et al. 2004). Adipocytes are the major cell type of the fat body in insects and are characterized morphologically by the presence of lipid droplets, glycogen rosettes and protein granules (Dean et al. 1985; Willott et al. 1988; Arrese and Soulages 2010; Lipovšek et al. 2011). However, cockroaches (except

for *Nocticolidae*) have two additional cell types in the fat body, namely urocytes and mycetocytes (Downer 1982; Locke 1984; Lo et al. 2007). Urocytes are specialized for urate storage with characteristic vacuoles or units having a fibrous cortex and characteristic cores (Downer 1982; Sobotník et al. 2006; Arrese and Soulages 2010; Lipovšek et al. 2011; Park et al. 2013). Cockroaches such as *Periplaneta americana* store uric acid, which is considered to be a nitrogen resource for amino acid synthesis upon low- or no-protein food conditions (Mullins 1974; Mullins and Cochran 1975a, 1975b; Cochran et al. 1979; Cochran 1985). Mycetocytes maintain an endosymbiont, *Blattabacterium cuenoti*, which inhabits not only the fat body but also the ovaries and embryos (Hollande and Favre 1931; Brooks 1970). This endosymbiont contributes to the synthesis of essential nutrients such as amino acids, an example being the aphid endosymbiont *Buchnera* (Brooks and Richards 1955; Henry 1962; Douglas 1998). *B. cuenoti* uses urea and ammonia, which are metabolites of uric acid, for amino acid synthesis (Sabree et al. 2009). The presence of both urocytes and mycetocytes might complement the roles of autophagy in recycling amino acids in the fat body or other organs of cockroaches under starvation.

In the midgut of arthropods, starvation stimulates the expression of *Atg8*, for example, in the tick *Haemaphysalis longicornis* (Umemiya-Shirafuji et al. 2010) and the wax moth *Galleria mellonella* (Khoa and Takeda 2012). In *P. americana*, starvation over 2 weeks reduces survival and increases the appearance of apoptosis in the nidi, which are the nests of stem cells producing the new midgut epithelium (Park et al. 2009, 2013). However, whether autophagy is induced in the midgut of starved cockroaches before or after the massive death and explosive increase of apoptosis has not been established. Autophagy is also observed in the remodeling of the larval midgut of the silk worm, *Bombyx mori*, during metamorphosis and Franzetti et al. (2012) pointed out that the remodeling of the tissues involves a combination of autophagy initially and apoptosis subsequently.

In the present study, we cloned a cDNA encoding an *Atg8* homolog from *P. americana* and determined the amino acid sequence of Atg8 of *P. americana*, *Pa*Atg8. On the basis of this sequence, we designed a *Pa*Atg8 antibody (Shelly et al. 2009). The presence and amounts of the Atg8-II form were monitored as an autophagic marker both in the fat body and in the midgut of the starved cockroaches by immunoblotting with the *Pa*Atg8 antibody, because the amount of Atg8-II is clearly correlated with the number of autophagosomes (Mizushima and Yoshimori 2007). Ultrastructurally, the presence of autophagic compartments, namely, autophagosomes and autolysosomes, was observed and quantified in each of the three types of fat body cell (trophocytes, urocytes and mycetocytes), in columnar cells, which are major components of the midgut epithelium and in the nidi, by electron microscopy. In the trophocytes, we also quantified the presence of protein granules, derived from the hemolymph proteins that have been taken up, at this time (Locke and Collins 1968; Locke 1984). Acid phosphatase activity was investigated as lysosomal activity in both the tissues, because autolysosomes are a combination of autophagosomes and lysosomes (Franzetti et al. 2012). Our aim is thus to characterize the roles of autophagy in adaptation to starvation with regard to the fat body and midgut of *P. americana*.

Materials and methods

Insects

Stock colonies of *P. americana* were maintained in terms of mass on an artificial diet (MF, ORIENTAL YEAST, Tokyo, Japan) with water provided ad libitum, at 25 °C, under light:dark (LD) 12:12. Newly emerged adult males collected from the colonies were kept together in plastic containers (30.0×16.5×13.5 cm) for 1 week. Each container housed 15–18 cockroaches that had constant access to the artificial diet and water. The cockroaches were transferred to small plastic cups (diameter: 10.0 cm, height4.5 cm) that were individually placed for several weeks at 25 °C under LD 12:12. Control roaches were fed normally, whereas the experimental animals were deprived of food.

Cloning and sequence analysis of *Pa*Atg8

Total RNA was extracted from the ventral nerve cords of fed cockroaches according to the manufacturer's instructions (ISOGEN, NIPPON GENE, Japan), because the massive lipids and glycogen in the fat body disturbed the extraction by the solution. A cDNA library was constructed from the total RNA by using ReverTra Ace (TOYOBO, Japan) and random primers. The partial sequence of *Atg8* of *P. americana* was amplified with the first degenerate primer pair (forward primer, 5′-CCNGTNATHGTNGARAARGCNCCNAA-3′; reverse primer, 5′-GTNGGNGGDATNAYRTTRTTNACRAA-3′). The amplification was performed by using 5 cycles, each consisting in 94 °C for 30 s, 55–50 °C for 30 s and 72 °C for 2 min followed by 30 cycles each consisting in 94 °C for 30 s, 50 °C for 30 s and 72 °C for 2 min and a final extension at 72 °C for 10 min. The first-round polymerase chain reaction (PCR) products were reamplified by using the second degenerate primer pair (forward primer, 5′-CCNGTNATHGTNGARAARGCNCCNAA-3′; reverse primer, 5′-GGDATNAYRTTRTTNACRAARAARAA-3′). The amplification was performed by using five cycles each consisting in 94 °C for 30 s, 54–49 °C for 30 s and 72 °C for 2 min followed by 30 cycles each consisting in 94 °C for 30 s, 49 °C for 30 s and 72 °C for 2 min and a final extension at

72 °C for 10 min. The resulting product was purified by using the Qiaquick Gel Extraction kit (GE Healthcare Life Sciences, UK) and subcloned into the pT7 blue vector (NOVAGEN, USA and Canada) by using Ligation High (TOYOBO). The DNA inserts of the positive clones were amplified by PCR with pT7 blue vector primers (forward primer, 5′-ATGACC ATGATTACGCCAAG-3′; reverse primer, 5′-GTTTTCCC AGTCACGAC-3′). The single-stranded cDNA for 5′/3′ RACE PCR was synthesized with the anchor primer supplied in the SMARTer RACE cDNA Amplification Kit (Clontech, USA). All primers were ordered from Invitrogen (USA) and all PCR experiments were performed by using Advantage 2 Polymerase Mix (Clontech) and 0.25 mM deoxynucleotide triphosphate on a thermal cycler (model Gene Amp PCR system 9600; Applied Biosystems, USA).

DNA sequencing was performed by using a 3100 Genetic Analyzer (Applied Biosystems) with the BigDye Cycle Sequencing Terminator System (Applied BioSystems) and then analyzed with Genetyx (Genetic Information Processing Software, Tokyo, Japan) or Bio Edit (Biological Sequence Alignment Editor, Ibis Therapeutic, Carlsbad, Calif., USA). The deduced amino acid sequence was checked for homology with other Atg8 sequences by using a FASTA homology search in the databases of the National Center for Biotechnology Information (NCBI).

Antibody

Polyclonal rabbit anti-*Pa*Atg8 antibody for immunoblotting was generated against a peptide sequence (FEKRKAEGEKIRRKYPDR) by Genemed Synthesis (Texas, USA) as referenced from the Atg8 antibody for *D. melanogaster* (Shelly et al. 2009).

Immunoblotting

Sample preparation and blotting followed the protocol of Abcam (www.abcam.com/technical; USA). Fat bodies or midguts (50 mg) collected from 3–5 cockroaches were homogenized in 500 μl modified RIPA buffer consisting of 150 mM sodium chloride, 1.0 % Triton X-100, 0.5 % sodium deoxycholate, 0.1 % SDS, 1 mM phenylmethane sulfonylfluoride (PMSF), 50 mM TRIS, pH 8.0. After homogenization, the tissues were agitated for 2 h at 4 °C and then centrifuged for 20 min (10,000*g*, 4 °C). The supernatant, whose protein concentration was checked by using a BCA Protein Assay Kit (Thermo Fisher Scientific, Yokohama, Japan), was adjusted to 5 μg/μl, diluted twice in Laemmli buffer (4 % SDS, 10 % 2-mercaptoethanol, 20 % glycerol, 0.004 % bromophenol blue, 0.125 M TRIS–HCl) and boiled for 5 min. The samples were subsequently kept for 5 min at room temperature and then stored at −20 °C before SDS-polyacrylamide gel electrophoresis (SDS-PAGE). A total of 20 μg protein applied to each lane was separated on a 15 % gel by SDS-PAGE and then blotted onto a polyvinylidene difluoride (PVDF) transfer membrane (0.45 μm pore size; Millipore, USA). As an internal standard, replicated gels were stained with Coomassie Brilliant Blue (CBB) to check the amount of applied proteins (Welinder and Ekblad 2011; Franzetti et al. 2012).

Non-specific binding was blocked by using 5 % skim milk powder (MEGMILK SNOW BRAND, Japan) dissolved in TTBS (0.05 M TRIS–HCl, 0.25 M NaCl, pH 7.0 containing 0.1 % Tween 20). After being blocked, membranes were washed three times with TTBS and incubated at 4 °C overnight in *Pa*Atg8 primary antibody solution diluted 1:10,000 in TTBS containing 1 % bovine serum albumin (Nacalai Tesque, Japan). As a negative control, preimmune rabbit serum was incubated instead of the anti-*Pa*Atg8 antibody. After incubation, the membranes were washed 3 times in TTBS and incubated in horseradish-peroxidase-conjugated donkey anti-rabbit secondary antibody (GE Healthcare Life Sciences) diluted at 1:2000 for 1 h at room temperature. After incubation, membranes were rinsed in TTBS and then allowed to react with ECL Western blotting detection reagents (ECL Prime, GE Healthcare Life Sciences). Bands were detected by using ImageQuant LAS 4000 (GE Healthcare Life Sciences). The protein sizes were estimated by using protein markers (Bio-Rad Laboratories, USA).

Electron microscopy

Dissected fat bodies or midguts were fixed in 2.5 % glutaraldehyde (GA) in Millonig's phosphate buffer (M-PBS). Five minutes later, the tissues were cut into small cubes (1 mm× 1 mm×1 mm), transferred into a new container and fixed in fresh GA solution at 4° C overnight. The tissue cubes were rinsed in M-PBS 3 times for 10 min each, fixed with buffered 1 % osmium tetroxide for 1 h at 4° C, dehydrated in ethanol and embedded in Quetol 812 resin mixture. Ultrathin sections were cut from the resin blocks with an ultra-microtome MT-1 (Ivan Sorvall) by using a histo-diamond knife or diamond knife (Diatome, Switzerland). The sections on 100 mesh grids (VECO, Holland) were stained with 4 % uranyl acetate for 10 min and lead citrate for 10 min and were then observed by using an H-7100 electron microscope (Hitachi, Japan) or a JEM-1400 (JEOL DATUM, Japan) at 80 kV.

Morphometric analysis

In the fat body, trophocytes, urocytes and mycetocytes were photographed at a magnification of ×1000 at random (H-7100). The negatives were enlarged 13 times and printed. The proportion of the total area of each of the three different cell types that was occupied by autophagic compartments not related to the degraded endosymbionts was calculated (Weibel

1979, 1980). In trophocytes, the proportion of the total area that was occupied by protein granules was also calculated. The means and standard errors were obtained from measurements within 56 trophocytes, 12 mycetocytes and 23 urocytes from three samples per treated group.

In the midgut epithelium, one picture was taken at ×5000 magnification on a chosen grid. After being photographed, the field in the charge-coupled device camera (JEM-1400) was moved a distance of 18.6 μm and then photographed at the same magnification once again. The whole area of the epithelium on the grid from microvilli to basal membrane, except for nidi and a total of 47–69 positions were photographed at random from three samples per treated group. Eight to fourteen nidi, which were chosen randomly from three to four samples, were also photographed at 1500× or 2000× magnification. The pictures were printed and the proportion of the total area of columnar cells or nidi that was occupied by autophagic compartments was calculated by a point-counting method (Weibel 1979, 1980). The means and standard errors were obtained from measurements within 69 pictures for columnar cells or 14 pictures for nidi.

Acid phosphatase activity

Fat bodies or midguts (50 mg) collected from two to four cockroaches were homogenized in 100 mM HEPES buffer (pH 5.0) containing 1 mM PMSF. The tissues were then centrifuged for 20 min (10,000*g*, 4 °C) and the supernatant was divided into tubes and stored at −80 °C before the assay. The protein concentration in the supernatant was determined by using the BCA Protein Assay Kit. The acid phosphatase activity in 20 μl supernatant was assayed on 96-well plates with 10 μl HEPES buffer and 20 μl 4-nitrophenyl phosphate as a substrate (5 mM) for 20 min, according to the modified methods of Moss (1983) and Franzetti et al. (2012) and the protocols of Abcam (ab83367, Acid Phosphatase Assay Kit) and the Cayman Chemical Company (10008051, Acid Phosphatase Assay kit). The reaction was performed at 37 °C and stopped with 100 μl 0.5 M sodium hydroxide. The chromogenic reaction was determined at 405 nm by using a Micro-plate reader (BioRad Model 550, Bio-Rad Laboratories). To convert the measurements into relative activity, mean values based on three to five measurements in the various samples (adjusted per milligram of protein concentration) from cockroaches before starvation were designated as 1.0.

Statistical analysis

Multiple comparisons between groups were performed by the Tukey-Kramer method for morphometric analysis. Statistically significant differences were determined by a *t*-test for acid phosphatase activity between the starved and unstarved treatments at the same time points (StatView 5.0 software Japanese version, SAS Institute, USA).

Results

cDNA cloning and sequence analysis of *Pa*Atg8

cDNA encoding an Atg8 homolog was cloned from the ventral nerve cord of *P. americana* by means of a degenerate PCR strategy with oligonucleotide primers based on conserved amino acid sequences from Atg8 homologs of other insects and a budding yeast (*PaAtg8*; ID accession: AB856588). The amplified 896-bp cDNA was not the full sequence but covered all of the coding region. This cDNA was composed of a short 5′ untranslated sequence of 87 bp, a single open reading frame (ORF) of 351 bp and a 3′ untranslated sequence of 458 bp (Fig. 1a). The ORF region began with a start codon at position 88 and terminated with a TAA stop codon at position 441. The deduced sequence was 117 amino acids long, with a molecular weight of 14 kDa (Genetyx).

An alignment (Fig. 1b) and a BLAST search (Table 1) indicated that the amino acid sequence had high identity with the Atg8 of other insects such as *D. melanogaster* (97 %, NP 727447), *B. mori* (96 %, NP 001040244) and *Apis mellifera* (90 %, XP 001120069). The sequence had low identity with the Atg8 of *Saccharomyces cerevisiae* (59 %, NP 009475) and with LC3, which is microtubule-associated protein 1-light chain 3 and functions as Atg8 in mammals, of *Homo sapiens* (32 %, NP 115903) and *Mus musculus* (32 %, NP 080011).

Presence of Atg8-II

The presence of Atg8-II in the fat body and midgut was examined by immunoblotting under starvation and under continuous feeding to assess the onset of the autophagic pathway. *Pa*Atg8-I and *Pa*Atg8-II bands were localized between 15 and 20 kDa on the PVDF membrane (Fig. 2a, b). In the fat body, starvation slightly reduced *Pa*Atg8-I and increased *Pa*Atg8-II (Fig. 2a). Continuous feeding showed no

Fig. 1 Sequence analysis of *Pa*Atg8. **a** Nucleotide sequence of the cDNA encoding *Atg8* isolated from *Periplaneta americana* and the deduced amino acid sequence (*asterisk* stop codon). The C-terminal glycine residue *underlined* is tethered to phosphatidylethanolamine. **b** Comparison of amino acid sequences of *Pa*Atg8 with Atg8 of other insects, the fruit fly (*Drosophila melanogaster*), silk worm (*Bombyx mori*) and honeybee (*Apis mellifera*). Amino acid sequences are available from the NCBI/GenBank database (*asterisks* identical residues). The peptide sequence for *Pa*Atg8 antibody production is *boxed*. Tyr49 and Leu50, which are required for activation of the lipidated form of Atg8 by Atg7 and Atg3, are *boxed in red*. Phe77 and Phe 79, which are parts of the recognition site for Atg4, are *boxed in blue*

a

```
TTCGTGCTTGTGGATTGATTGTTGTCAGTACTCCATAACAGCAAAATTATTAGCTAAAGC  60

TTACAAATAGTGTATGCCTTTGAAAACATGAAATTCCAATACAAGGAAGAACATCCATTC  120
                          M  K  F  Q  Y  K  E  E  H  P  F

GAAAAGAGGAAGGCCGAGGGAGAAAAAATTAGGAGAAAATATCCTGACAGAGTTCCCGTA  180
 E  K  R  K  A  E  G  E  K  I  R  R  K  Y  P  D  R  V  P  V

ATTGTGGAAAAAGCCCCTAAAGCAAGAATTGGAGATCTCGATAAGAAGAAGTACCTGGTT  240
 I  V  E  K  A  P  K  A  R  I  G  D  L  D  K  K  K  Y  L  V

CCATCAGATCTGACAGTAGGCCAGTTCTACTTCCTCATCAGGAAGAGGATTCACCTACGT  300
 P  S  D  L  T  V  G  Q  F  Y  F  L  I  R  K  R  I  H  L  R

CCTGAGGATGCATTATTTTTCTTCGTCAACAATGTAATTCCCCCTACAAGTGCCACTATG  360
 P  E  D  A  L  F  F  F  V  N  N  V  I  P  P  T  S  A  T  M

GGTTCTCTCTACCAGGAGCACCATGAGGAAGATTTCTTCCTTTACATCGCTTACAGTGAT  420
 G  S  L  Y  Q  E  H  H  E  E  D  F  F  L  Y  I  A  Y  S  D

GAGAATGTTTATGGCCAGTAAATCATCTTGCTCCCCTGCTTCAGTTTTTTTTTCTCCCGC  480
 E  N  V  Y  G  Q  *

CACAGATGAATAAATATTATGTGACATAGGTTATGAAGAACGTTGCAGATTGGAGTGATA  540

CTTGTCTTTTTTACTTTTCCATGATCAAGCATTTGTTTAGAAAGATAAGGAAATAGTATT  600

TTATGCTGTATTCCGTATTATTATAAATTTCAGTATTTCTTTTCTTTTTTGGTGGACATA  660

TTAGTTAAACTTCTTTCTTTCCTCAGAATATATTCACATTTGATTATGGCTGTAGGATTA  720

CTTTTATTTCCTTCAATATGTAGCACATTAATTGCAAATATTTAATTTTAAAAATCAGTT  780

TTAAGAATTCTTATCCATCAACTATTAATATACTATATTATATACTACAAGGATGGAATG  840

TATATAAGTAATGTATACAGTGGTATAAATAAATAAATTTCATTTTAGAAAAAAAA      896
```

b

```
Drosophila      MKFQYKEEHAFEKRRAEGDKIRRKYPDRVPVIVEKAPKARIGDLDKKKYL 50
Periplaneta     MKFQYKEEHFFEKRKAEGEKIRRKYPDRVPVIVEKAPKARIGDLDKKKYL 50
Bombyx          MKFQYKEEHSFEKRKAEGEKIRRKYPDRVPVIVEKAPKARLGDLDKKKYL 50
Apis            MKFHYKEKHSFERRKVEGEKIRRKYPERVPVIVEKAPKAKISDLDKQKYL 50
                ***:***:*.**:*:.**:*******:************:::****:***

Drosophila      VPSDLTVGQFYFLIRKRIHLRPEDALFFFVNNVIPPTSATMGSLYQEHHE 100
Periplaneta     VPSDLTVGQFYFLIRKRIHLRPEDALFFFVNNVIPPTSATMGSLYQEHHE 100
Bombyx          VPSDLTVGQFYFLIRKRIHLRPEDALFFFVNNVIPPTSATMGSLYQEHHD 100
Apis            VPSDLTVGQFYFLIRKRIHLRPEDALFFFVNNIIPPTSATMGSLYAEHHE 100
                ********************************:************ ***:

Drosophila      EDYFLYIAYSDENVYGMAKIN 121
Periplaneta     EDFFLYIAYSDENVYGQ---- 117
Bombyx          EDFFLYIAFSDENVYGN---- 117
Apis            EDFFLYIAYSDENVYGH---- 117
                **:*****:*******
```

Table 1 Identity in deduced amino acid sequences of *Pa*Atg8 with Atg8 of other insects and yeast or LC3 (microtubule-associated protein 1-light chain 3) of mammals

Species	Accession number	Identity
Drosophila melanogaster	(NP 727447)	97 %
Bombyx mori	(NP 001040244)	96 %
Apis mellifera	(XP 001120069)	90 %
Saccharomyces cerevisiae	(NP 009475)	59 %
Homo sapiens (LC3)	(NP 115903)	32 %
Mus musculus (LC3)	(NP 080011)	32 %

tendency to increase or decrease *Pa*Atg8-I and *Pa*Atg8-II (Fig. 2a). In the midgut, however, starvation strongly increased *Pa*Atg8-I gradually but *Pa*Atg8-II rapidly, over 2 weeks (Fig. 2b). Continuous feeding also strongly increased *Pa*Atg8-I but not *Pa*Atg8-II (Fig. 2b). Some weak immunopositive bands were observed below 15 kDa under both nutritional conditions. Preimmune rabbit serum showed no bands of *Pa*Atg8-I and *Pa*Atg8-II in either the fat body or midgut (data not shown). CBB staining showed no significant difference in protein bands from 15 to 20 kDa (data not shown).

Ultrastructural observation and quantification

Trophocytes, major components of fat body, contained lipid droplets and electron-dense protein granules that lay in the granular cytoplasm that shows stored glycogen (Fig. 3a, b). Mycetocytes are centrally located in the fat body lobes and contained an endosymbiont, *B. cuenoti* (arrowhead in Fig. 3a). Urocytes in the vicinity of mycetocytes had urate vacuoles, which had a fibrous cortex and a characteristic core (Fig. 3a). Starvation for 2 weeks eliminated protein granules in trophocytes (Fig. 3c) and reduced the proportion of the total area occupied by the granules in the cells (Fig. 4a). However, the proportion recovered to half of the original level after 4 weeks. The formation of autophagic compartments showing electron-dense and non-electron-dense areas and enveloping mitochondrion-like structures was stimulated in trophocytes (Fig. 3c, d) and urocytes (Fig. 3e) and the proportion of the total area occupied by the compartments increased in both the cell types over 2 weeks of starvation (Fig. 4b). However, urocytes did not show a statistically significant increase ($P>0.05$, Tukey-Kramer method). Mycetocytes did not show autophagic compartments similar to those observed in trophocytes, even under starvation (Fig. 3c).

Columnar cells, which were major components of the midgut epithelium, were cylindrical in shape and characterized morphologically by the presence of microvilli (Fig. 5a). Nidi were located on the basal membrane of the epithelium and characterized by multilayered packed cells (Fig. 5a). Starvation stimulated the appearance of autophagic compartments in the columnar cells (Fig. 5b), autophagosomes delineated by double membranes (arrows in Fig. 5c) and autolysosomes showing electron-dense myelin-like structures (arrowhead in Fig. 5c), or denaturing rough endoplasmic reticulum (arrow in Fig. 5d) and increased the proportion of the total area occupied by the compartments in the cells (Fig. 6a). Four weeks of starvation changed the structure of some nidi from the multilayered packed type into the papilla-shaped form (Fig. 5e) and stimulated the appearance of autolysosomes in the nidi (arrowhead in Fig. 5e). The proportion of the total area occupied by the autophagic compartments in the nidi increased after 4 weeks (Fig. 6b) but this increase was not statistically significant ($P>0.05$, Tukey-Kramer method). Apoptotic bodies, which had condensed chromatin enveloped by nuclear membrane (arrows in Fig. 5e), were also observed near the compartments (arrowhead in Fig. 5e).

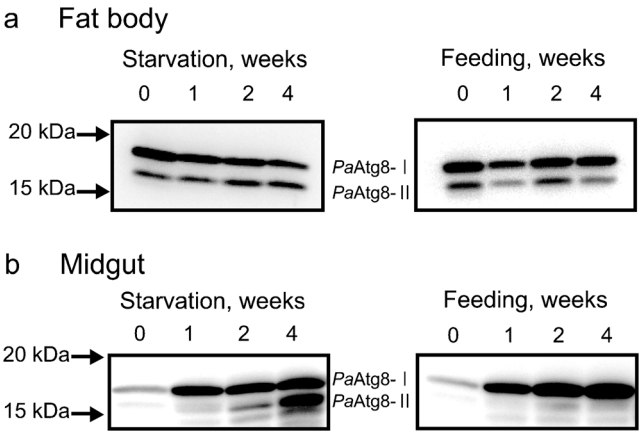

Fig. 2 Immunoblotting with *Pa*Atg8 antibody in the fat body (**a**) and midgut (**b**) under starvation and continuous feeding. **a** In the fat body, starvation slightly reduced *Pa*Atg8-I and increased *Pa*Atg8-II. Continuous feeding showed no tendency to increase or decrease either *Pa*Atg8-I or *Pa*Atg8-II. **b** In the midgut, starvation and continuous feeding increased *Pa*Atg8-I but *Pa*Atg8-II was increased only after 2 weeks of starvation. *Pa*Atg8-I and *Pa*Atg8-II bands are found between 15 and 20 kDa. Some weak immunopositive bands were observed below 15 kDa under both nutritional conditions. The *numbers above the lanes* indicate the number of weeks of starvation or feeding

Comparison of acid phosphatase activity

Acid phosphatase activities per milligram of protein in the fat body and midgut were investigated under starvation and continuous feeding. In the fat body, the enzymatic activity increased slightly after 1 week of starvation but showed no significant difference from that of fed cockroaches ($P>0.05$, Fig. 7a). In the midgut,

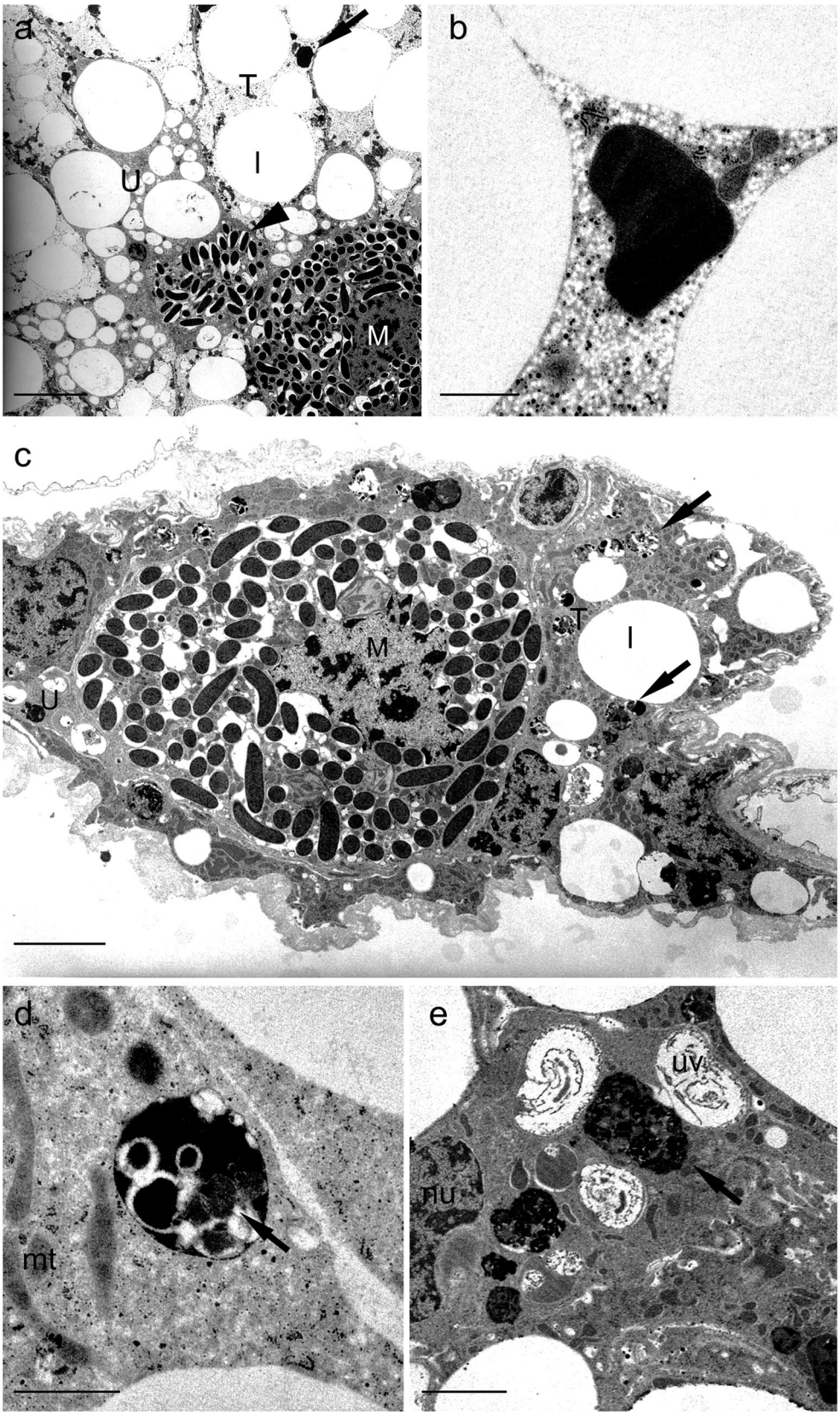

Fig. 3 Ultrastrucuture of fat body lobe of *P. americana*. **a** Fat body lobe of fed cockroaches. Trophocytes (*T*), urocytes (*U*) and mycetocytes (*M*) were observed (*l* lipid droplet, *arrow* protein granule, *arrowhead* endosymbiont *Blattabacterium cuenoti*). **b** Magnifed protein granule showing electron-dense body in trophocytes. **c** Fat body lobe of cockroaches starved for 4 weeks. Formation of autophagic compartments was stimulated (*arrows*). **d** Magnified autophagic compartment (*mt* mitochondria). Mitochondrion-like structure was observed in the compartment (*arrow*). **e** Urocytes of cockroaches starved for 4 weeks (*arrow* autophagic compartment, *nu* nucleus, *uv* urate vacuole). *Bars* 10 μm (**a**), 1 μm (**b**, **d**), 5 μm (**c**), 2.5 μm (**e**)

starvation gradually reduced the enzymatic activity (Fig. 7b) and the activity in fed cockroaches was significantly higher than that of starved animals at the same time points ($P<0.05$; *t-test*).

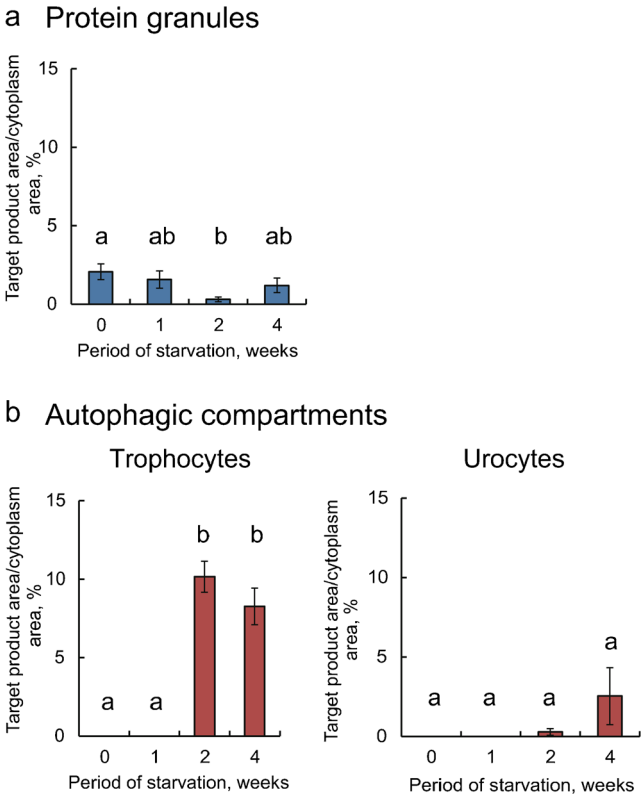

Fig. 4 Proportion of the total area occupied by protein granules (**a**) or autophagic compartments (**b**) in the trophocytes or urocytes under starvation. **a** The proportion occupied by protein granules in trophocytes was reduced after 2 weeks and recovered to half of the original level after 4 weeks of starvation. **b** Starvation increased the proportion occupied by atuophagic compartments in both trophocytes and urocytes. Each value is the mean of the measurements from 23–56 trophocytes and from 13–23 urocytes derived from three samples. *Error bars* indicate SE. *Different letters* indicate statistically significant differences between groups ($P<0.05$, Tukey-Kramer method)

Discussion

Atg8 is cleaved at the last residue by Atg4 leading to exposure of a C-terminal glycine residue (Atg8-I; Kirisako et al. 2000). This is activated by Atg7 and finally conjugated to PE by Atg3 (Kirisako et al. 2000; Ichimura et al. 2000; He and Klionsky 2009). Atg7 and Atg3 correspond to the E1 and E2 enzymes of the ubiquitination system, respectively. PE-conjugated Atg8, Atg8-II, becomes tethered in the membrane of autophagic compartments, as is required for the formation of an autophagosome (Kirisako et al. 1999; Kabeya et al. 2000; Amar et al. 2006; Nakatogawa et al. 2007). *Pa*Atg8 has a glycine residue at the 116th residue along its length of 117 amino acids and has two important conserved sites. Phe77 and Phe 79 are parts of the recognition site for Atg4 and Tyr49 and Leu50 form the site for activation of the lipidated form of Atg8 by Atg7 and Atg3 (Fig. 1b; Amar et al. 2006; Khoa and Takeda 2012). Conservation of these sites and high homology with the Atg8 of other insects, such as *D. melanogaster*, *B. mori* and *A. mellifera*, suggest that the cloned gene is Atg8 of *P. americana* (Table 1).

In the trophocytes of the fat body of *P. americana*, starvation reduces the proportion of the total area occupied by protein granules, derived from hemolyph proteins that have previously been taken up, after 2 weeks (Fig. 4a). The cave cricket, *Troglophilus neglectus*, stops feeding and the size of the protein granules in the tissues is much reduced during overwintering (Lipovšek et al. 2011). The reduction of the granules both in the cockroach and in the cricket implies a functional role of the granules in the storage of nutrients upon starvation. Although the proportion recovers to half of the original level after 4 weeks in the cockroach, another cave cricket, *T. cavicola*, exhibits a reduction in the size of protein granules from November to January, with a restoration of their size by March, during overwintering (Lipovšek et al. 2011). The recovery in *P. americana* and this cave cricket, *T. cavicola*, might be related to metabolic changes for the utilization of reserved nutrients.

Autophagy is a mechanism leading not only to the digestion of the cytoplasm for the recycling amino acids under amino acid deprivation (Rusten et al. 2004; Scott et al. 2004) but also to the formation of protein granules in the fat body during metamorphosis (Locke 1984). The protein granules fuse with autophagic vacuoles for the digestion of excessive membranes and the crystallization of stored proteins. The crystallized proteins are mobilized for the utilization of amino acids during development. In the fat body of *D. melanogaster*, the Aut1 mutant, namely, Atg3-loss-of-function larvae, fail to form autophagic vacuoles and protein granules before pupariation (Juhász et al. 2003). The absence of protein granules in these mutants implies that autophagy-related genes, *Atg* genes, are involved in the formation of protein granules. In fed cockroaches, although *Pa*Atg8-II is observed in the fat body (Fig. 2a), autophagic compartments were not observed in the three cell types and some large protein granules were observed in the trophocytes (Figs. 3a, 4a, b). Starvation reduces the protein granules and extensively stimulates the formation of autophagic compartments in the trophocytes (Fig. 4b) but slightly increases *Pa*Atg8-II in the fat body (Fig. 2a). These results imply that Atg8 is related not only to the induction of autophagy but also to the formation of protein granules in the trophocytes in *P. americana* under starvation and continuous feeding, respectively. The crystallization of protein granules via the fusion with autophagic vacuoles might explain the high acid phosphatase activity in the fat body of fed cockroaches (Fig. 7a).

Although the mycetocytes contain dying *B. cuenoti* that show an electron-dense outer layer and lose cytoplasm from the symbiosome membrane, instead of autophagic compartments, the death of the endosymbionts is not related to starvation (Park et al. 2013), unlike in the pea aphid, *Acyrthosiphon pisum*, which has a lysosomal digestion system

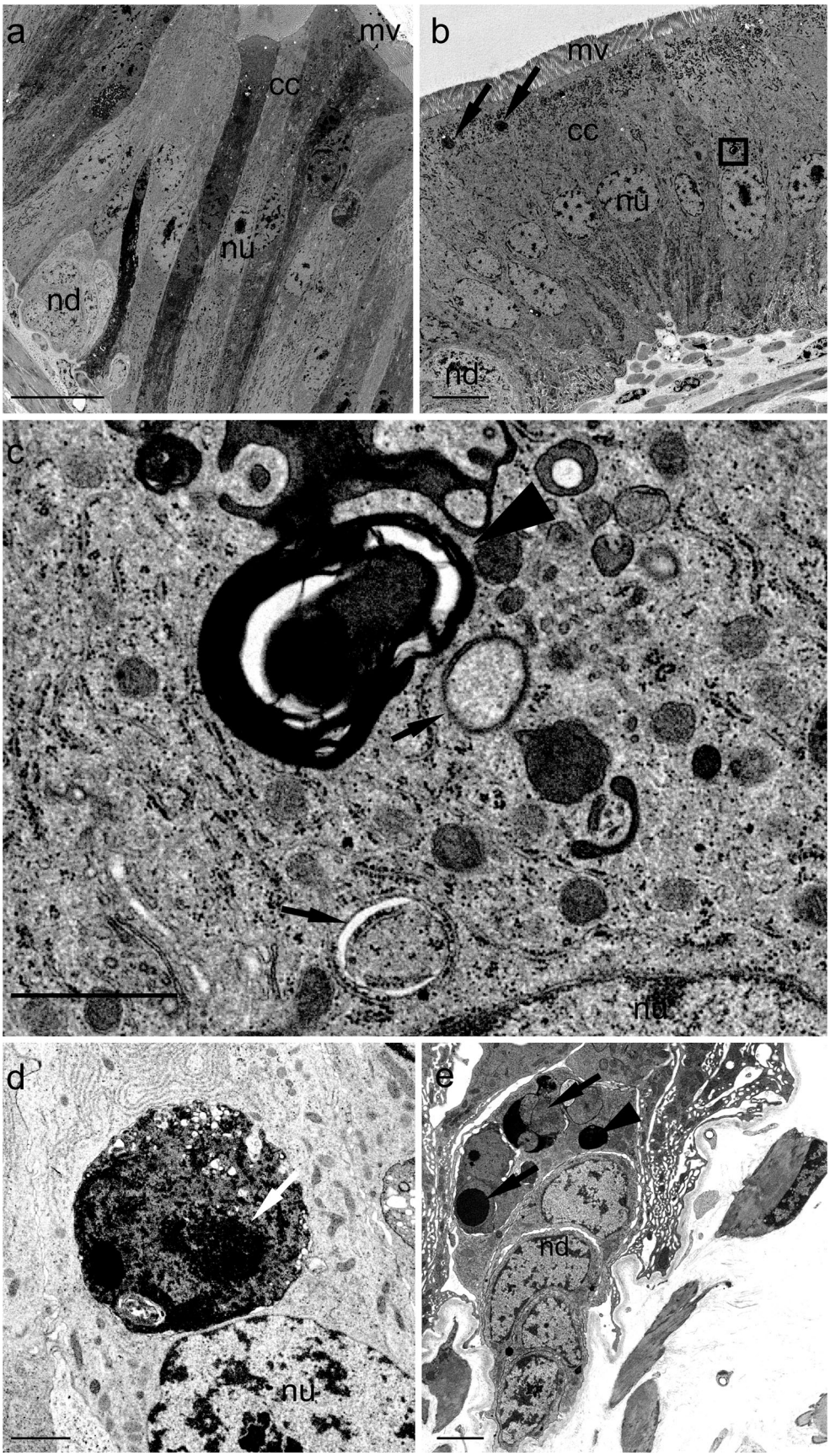

Fig. 5 Ultrastrucuture of midgut epithelium of *P. americana*. **a** Midgut epithelium of fed cockroach. Columnar cells (*cc*) and a nidus (*nd*) are present (*mv* microvilli, *nu* nucleus). **b** Midgut epithelium of cockroach starved for 2 weeks. Some autolysosomes (*arrows*) were observed near microvilli (*mv*). **c** Higher magnification of the *boxed area* in Fig. **b**. Autophagosomes showing double membranes (*arrows*) and an autolysosome showing an electron-dense myelin-like structure (*arrowhead*) can be seen. **d** Autolysosome showing denatured rough endoplasmic reticulum (*arrow*) in the midgut epithelium of cockroaches starved for 4 weeks. **e** Papilla-shaped nidus showing an apoptotic body (*arrows*) and an autolysosome (*arrowhead*) in midgut epithelium of cockroach starved for 4 weeks. *Bars* 20 μm (**a**), 10 μm (**b**), 1 μm (**c**, **f**), 2 μm (**d**, **e**)

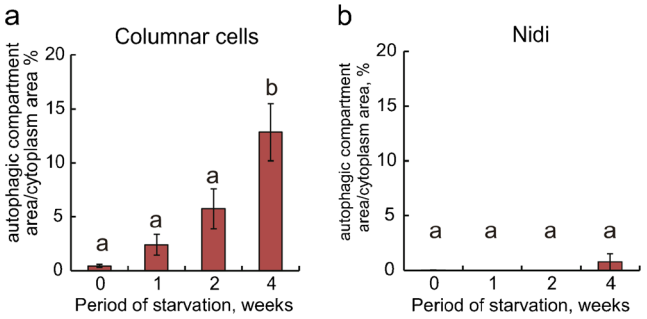

Fig. 6 Proportion of total area occupied by autophagic compartments in columnar cells (**a**) or nidi (**b**) from cockroaches under starvation. Starvation increased the proportion of the compartments in both cells but the increase in nidi was not statistically significant ($P>0.05$). Each value is the mean of the measurements from 47–69 positions in columnar cells derived from three samples and from 8–14 nidi derived from three to four samples. *Error bars* indicate SE. *Different letters* indicate statistically significant differences between groups ($P<0.05$, Tukey-Kramer method)

for *Buchnera* in its mycetocytes, as a source of nutrients for the developing flight muscle (Nishikori et al. 2009). Lysosomes fuse with the symbiosome membranes and then digest *Buchnera*. Lysosomal digestion systems such as autophagy or bacterial digestion might not be important for the mycetocytes of *P. americana* as a source of nutrients.

In the midgut of *P. americana*, starvation stimulates the appearance of autophagic compartments in the columnar cells and nidi (Fig. 6a, b). However, some autolysosomes might be engulfed together with digested debris of dead columnar cells or stem cells by neighboring cells, because it is impossible to distinguish ultrastructually which secondary lysosomes are derived from autophagy or endocytosis. TUNEL (TdT-mediated dUTP nick-end labeling)-positive products, which are smaller than those of the nuclei, were observed in columnar cells (Park et al. 2009) and apoptotic bodies showing condensed chromatin enveloped by nuclear membrane have been localized in the nidi near the autolysosomes (Fig. 5e). However, starvation increases Atg8-II in the midgut (Fig. 2b) and autophagosomes showing double membranes were observed in the columnar cells (Fig. 5c). Starvation increases Atg8 in the midgut epithelium of the wax moth, *G. mellonella* (Khoa and Takeda 2012) and the expression of *Atg8* in the midgut of the tick, *Haemaphysalis longicornis*, with the formation of autophagic vacuoles (Umemiya-Shirafuji et al. 2010). The present results and the reports from other arthropods show that not all autophagic compartments in the columnar cells are derived from engulfed cell debris and that starvation stimulates autophagy in the cells.

During metamorphosis, acid phosphatase activity connected to lysosomes increases in the midgut, which is degraded by the combination of autophagy and apoptosis (Sass et al. 1989; Franzetti et al. 2012). However, feeding rather than starvation increases the activity of this enzyme in the midgut of *P. americana* (Fig. 7b). In the midgut, acid phosphatase is localized in the cytoplasm for the digestion of food (Srivastava and Saxena 1967; Cheung and Low 1975; Terra et al. 1979). The Colorado potato beetle, *Leptinotarsa decemlineata*, reared under short-day conditions, shows reduced activity of the enzyme in the midgut after the cessation of feeding for diapause (Yi and Adams 2001). The characteristics of the enzyme, which is related to feeding behavior, might explain the high activity in the midgut of the fed cockroaches.

Autophagy is induced rapidly in the fat body of larval fruit fly, *D. melanogaster* (Rusten et al. 2004) and adult cockroach, *P. americana* (Fig. 4b), within a day and over 2 weeks of starvation, respectively. The late induction of autophagy in the cockroach might be caused by the delayed exhaustion of amino acids, which are metabolized from the stored uric acid in the fat body, because our previous study showed the

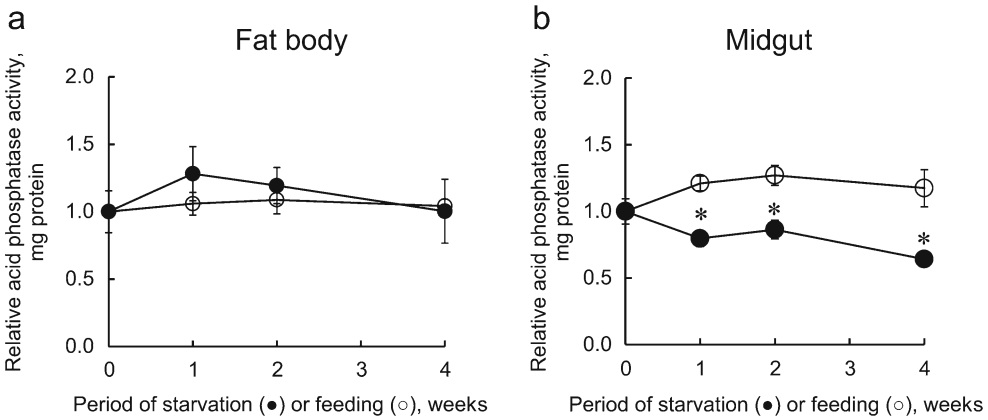

Fig. 7 Comparison of acid phosphatase activity per milligram of protein in the fat body (**a**) and midgut (**b**) of cockroaches under starvation (*filled circles*) and continuous feeding (*empty circles*). **a** In the fat body, 1 week of starvation lead to a slight increase in activity but this was not significantly different from that of fed cockroaches. **b** In the midgut, starvation reduced the enzymatic activity gradually but continuous feeding maintained higher activity than that in the starved animals. To convert the measurements into relative activity, mean values based on 3–5 measurements, which were adjusted per milligram of protein, from cockroaches before starvation were expressed as 1.0 (*asterisks* statistically significant difference from the fed control at the same time point, $P<0.05$; *t-test*)

rapid size reduction of urate vacuoles of *P. americana* during a week of starvation (Park et al. 2013). In a wood-eating termite, *Reticulitermes flavipes*, uric acid is transported from the hemolymph, via the Malpighian tubules, to the hindgut in which uric acid is metabolized into ammonia by gut bacteria (Potrikus and Breznak 1980a, 1980b, 1981). The genome of *B. cuenoti* does not contain any genes encoding uricolytic enzymes such as uricase and xanthine dehydrogenase, which degrade uric acid but it is capable of metabolizing urea or ammonia, from which almost all amino acids are synthesized, with the exceptions of glutamine and asparagine (Sabree et al. 2009). The metabolic analysis of the termite and the genomic analysis of *B. cuenoti* suggest that *P. americana* metabolizes the stored uric acid into amino acids by the combination of gut symbionts (Donnellan and Kilby 1967) and *B. cuenoti*. Antibiotics, which kill gut symbionts or endosymbionts, slow the metabolism of uric acid in the whole tissues of the brown plant hopper, *Nilaparvata lugens* (Hongoh and Ishikawa 1997) and affect the composition of amino acids in the hemolymph of the shield bug, *Parastrachia japonensis* (Kashima et al. 2006). The rapid increase of autophagy in the midgut over 2 weeks of starvation (Figs. 2b, 6a) follows the rapid size reduction of the urate vacuoles (Park et al. 2013) and might be caused by the exhaustion of amino acids provided by symbionts, especially glutamine and leucine in the hemolymph, because both amino acids are related to the suppression of autophagy by the activation of TOR, a target of rapamycin (Nicklin et al. 2009). The roles of the stored uric acid and gut symbionts or endosymbionts for the synthesis of amino acids should be investigated further, because they might be up-regulators of autophagy in the tissues of cockroaches.

In conclusion, long-term rather than short-term starvation over 2 weeks induces autophagy in the fat body and midgut of the American cockroach, *P. americana*, with autophagic profiles in these organs being distinct because of the presence or absence of an endosymbiont, *B. cuenoti*. The late induction of autophagy in the tissues might be related to synthesized amino acids by the combination of urocytes and mycetocytes in the fat body.

Acknowledgement We thank Prof. Pyoyun Park for advice and technical assistance with the electron microscopic observations.

References

Amar N, Lustig G, Ichimura Y, Ohsumi Y, Elazar Z (2006) Two newly identified sites in the ubiquitin-like protein Atg8 are essential for autophagy. EMBO Rep 7:635–642

Arrese EL, Soulages JL (2010) Insect fat body: energy, metabolism, and regulation. Annu Rev Entomol 55:207–225

Barth JM, Szabad J, Hafen E, Köhler K (2011) Autophagy in *Drosophila* ovaries is induced by starvation and is required for oogenesis. Cell Death Differ 18:915–924

Brooks MA (1970) Comments on classification of intracellular symbiotes of cockroaches and description of the species. J Invertebr Pathol 16: 249–258

Brooks MA, Richards AG (1955) Intracellular symbiosis in cockroaches. I. Production of aposymbiotic cockroaches. Biol Bull 109:22–39

Cheung WWK, Low KW (1975) Ultrastructural and functional differentiation of the midgut of the sugar cane beetle, *Protaetia acuminate* (F.) (Coleoptera: cetonidae). Int J Insect Morphol Embryol 4:349–361

Cochran DG (1985) Nitrogen excretion in cockroaches. Annu Rev Entomol 30:29–49

Cochran DG, Mullinus ED, Mullins KJ (1979) Cytological changes in the fat body of the American cockroach, *Periplaneta americana*, in relation to dietary nitrogen levels. Ann Entomol Soc Am 72:197–205

Dean RL, Collins JV, Locke M (1985) Structure of the fat body. In: Kerkut GA, Gilbert LI (eds) Comprehensive insect physiology, biochemistry, and pharmacology. Pergamon, New York, pp 155–210

Donnellan JF, Kilby BA (1967) Uric acid metabolism by symbiotic bacteria from the fat body of *Periplaneta americana*. Comp Biochem Physiol 22:235–252

Douglas AE (1998) Nutritional interactions in insect-microbial symbioses: aphids and their symbiotic bacteria *Buchnera*. Annu Rev Entomol 43:17–37

Downer RGH (1982) Fat body and metabolism. In: Bell WJ, Adiyodi KG (eds) The American cockroach. Chapman and Hall, New York, pp 151–174

Franzetti E, Huang ZJ, Shi YX, Xie K, Deng XJ, Li JP, Li QR, Yang WY, Zeng WN, Casartelli M, Deng HM, Cappellozza S, Grimaldi A, Xia Q, Feng Q, Cao Y, Tettamanti G (2012) Autophagy precedes apoptosis during the remodeling of silkworm larval midgut. Apoptosis 17:305–324

Hanaoka H, Noda T, Shirano Y, Kato T, Hayashi H, Shibata D, Tabata S, Ohsumi Y (2002) Leaf senescence and starvation-induced chlorosis are accelerated by the disruption of an *Arabidopsis* autophagy gene. Plant Physiol 129:1181–1193

He C, Klionsky DJ (2009) Regulation mechanisms and signaling pathways of autophagy. Annu Rev Genet 43:67–93

Henry SM (1962) The significance of microorganisms in the nutrition of insects. Trans N Y Acad Sci 24:676–683

Hollande AC, Favre R (1931) La structure cytologique de *Blattabacterium cuénoti* (Mercier) N. G., symbiote du tissue adipeux des Blattides. C R Seances Soc Biol Fil 107:752–754

Hongoh Y, Ishikawa H (1997) Uric acid as a nitrogen resource for the brown planthopper, *Nilaparvata lugens*: studies with synthetic diets and aposymbiotic insects. Zool Sci 14:581–586

Ichimura Y, Kirisako T, Takao T, Satomi Y, Shimonishi Y, Ishihara N, Mizushima N, Tanida I, Kominami E, Ohsumi M, Noda T, Ohsumi Y (2000) A ubiquitin-like system mediates protein lipidation. Nature 408:488–492

Juhász G, Csikós G, Sinka R, Erdélyi M, Sass M (2003) The *Drosophila* homolog of Aut1 is essential for autophagy and development. FEBS Lett 543:154–158

Kabeya Y, Mizushima N, Ueno T, Yamamoto A, Kirisako T, Noda T, Kominami E, Ohsumi Y, Yoshimori T (2000) LC3, a mammalian homologue of yeast Apg8p, is localized in autophagosome membranes after processing. EMBO J 19:5720–5728

Kashima T, Nakamura T, Tojo S (2006) Uric acid recycling in the shield bug, *Parastrachia japonensis* (Hemiptera: *Parastrachiidae*), during diapause. J Insect Physiol 52:816–825

Khoa DB, Takeda M (2012) Expression of autophagy 8 (Atg8) and its role in the midgut and other organs of the greater wax moth, *Galleria*

mellonella, during metamorphic remodelling and under starvation. Insect Mol Biol 5:473–487

Kirisako T, Baba M, Ishihara N, Miyazawa K, Ohsumi M, Yoshimori T, Noda T, Ohsumi Y (1999) Formation process of autophagosome is traced with Apg8/Aut7p in yeast. J Cell Biol 147:435–446

Kirisako T, Ichimura Y, Okada H, Kabeya Y, Mizushima N, Yoshimori T, Ohsumi M, Takao T, Noda T, Ohsumi Y (2000) The reversible modification regulates the membrane-binding state of Apg8/Aut7 essential for autophagy and the cytoplasm to vacuole targeting pathway. J Cell Biol 151:263–276

Kovács AL, Molnár K, Seglen PO (1981) Inhibition of autophagic sequestration and endogenous protein degradation in isolated rat hepatocytes by methylated adenosine derivatives. FEBS Lett 134: 194–196

Lipovšek S, Novak T, Janžekovič F, Pabst MA (2011) Role of the fat body in the cave crickets *Troglophilus cavicola* and *Troglophilus neglectus* (Rhaphidophoridae, Saltatoria) during overwintering. Arthropod Struct Dev 40:54–63

Lo N, Beninati T, Stone F, Walker J, Sacchi L (2007) Cockroaches that lack *Blattabacterium* endosymbionts: the phylogenetically divergent genus *Nocticola*. Biol Lett 3:327–30

Locke M (1984) The structure and development of the vacuolar system in the fat body of insects. In: King RC, Akai H (eds) Insect ultrastructure, vol 2. Plenum, New York, pp 151–197

Locke M, Collins JV (1968) Protein uptake into multivesicular bodies and storage granules in the fat body of an insect. J Cell Biol 36:453–483

Meléndez A, Tallóczy Z, Seaman M, Eskelinen EL, Hall DH, Levine B (2003) Autophagy genes are essential for dauer development and life-span extension in *C. elegans*. Science 301:1387–91

Mizushima N, Yoshimori T (2007) How to interpret LC3 immunoblotting. Autophagy 3:542–545

Mizushima N, Yamamoto A, Matsui M, Yoshimori T, Ohsumi Y (2004) In vivo analysis of autophagy in response to nutrient starvation using transgenic mice expressing a fluorescent autophagosome marker. Mol Biol Cell 15:1101–1111

Mizushima N, Levine B, Cuervo AM, Klionsky DJ (2008) Autophagy fights disease through cellular self-digestion. Nature 451:1069–1075

Moss WD (1983) Acid phosphatase. In: Bergmeyer J, Grassi M (eds) Esterases, glycosidases, lyases, ligases, vol 4: methods of enzymatic analysis. Weinheim, Verlag-Chemie, pp 92–106

Mullins DE (1974) Nitrogen metabolism in the American cockroach: an examination of whole body and fat body regulation of cations in response to nitrogen balance. J Exp Biol 61:557–570

Mullins DE, Cochran DG (1975a) Nitrogen metabolism in the American cockroach. I. An examination of positive nitrogen balance with respect to uric acid stores. Comp Biochem Physiol 50A:489–500

Mullins DE, Cochran DG (1975b) Nitrogen metabolism in the American cockroach. II. An examination of negative nitrogen balance with respect to mobilization of uric acid stores. Comp Biochem Physiol 50A:501–510

Nakatogawa H, Ichimura Y, Ohsumi Y (2007) Atg8, a ubiquitin-like protein required for autophagosome formation, mediates membrane tethering and hemifusion. Cell 130:165–178

Nicklin P, Bergman P, Zhang B, Triantafellow E, Wang H, Nyfeler B, Yang H, Hild M, Kung C, Wilson C, Myer VE, MacKeigan JP, Porter JA, Wang YK, Cantley LC, Finan PM, Murphy LO (2009) Bidirectional transport of amino acids regulates mTOR and autophagy. Cell 136:521–534

Nishikori K, Morioka K, Kubo T, Morioka M (2009) Age- and morph-dependent activation of the lysosomal system and *Buchnera* degradation in aphid endosymbiosis. J Insect Physiol 55:351–357

Park MS, Park P, Takeda M (2009) Starvation induces apoptosis in the midgut nidi of *Periplaneta americana*: a histochemical and ultrastructural study. Cell Tissue Res 335:631–638

Park MS, Park P, Takeda M (2013) Roles of fat body trophocytes, mycetocytes and urocytes in the American cockroach, *Periplaneta americana* under starvation conditions: an ultrastructural study. Arthropod Struct Dev 42:287–295

Potrikus CJ, Breznak JA (1980a) Uric acid-degrading bacteria in guts of termites [*Reticulitermes flavipes* (Kollar)]. Appl Environ Microbiol 40:117–124

Potrikus CJ, Breznak JA (1980b) Anaerobic degradation of uric acid by gut bacteria of termites. Appl Environ Microbiol 40:125–132

Potrikus CJ, Breznak JA (1981) Gut bacteria recycle uric-acid nitrogen in termites: a strategy for nutrient conservation. Proc Natl Acad Sci U S A 78:4601–4605

Rost-Roszkowska MM, Vilimova J, Sosinka A, Skudlik J, Franzetti E (2012) The role of autophagy in the midgut epithelium of *Eubranchipus grubii* (Crustacea, Branchiopoda, Anostraca). Arthropod Struct Dev 3:271–279

Rusten TE, Lindmo K, Juhász G, Sass M, Seglen PO, Brech A, Stenmark H (2004) Programmed autophagy in the *Drosophila* fat body is induced by ecdysone through regulation of the PI3K pathway. Dev Cell 7:179–192

Sabree ZL, Kambhampati S, Moran NA (2009) Nitrogen recycling and nutritional provisioning by *Blattabacterium*, the cockroach endosymbiont. Proc Natl Acad Sci U S A 106:19521–19526

Sass M, Komuves G, Csikos G, Kovács J (1989) Changes in the activities of lysosomal enzymes in the fat body and midgut of two lepidopteran insects (*Mamestra brassicae* and *Pieris brassicae*) during metamorphosis. Comp Biochem Physiol 92A:285–289

Schworer CM, Shiffer KA, Mortimore GE (1981) Quantitative relationship between autophagy and proteolysis during graded amino acid deprivation in perfused rat liver. J Biol Chem 256:7652–7658

Scott RC, Schuldiner O, Neufeld TP (2004) Role and regulation of starvation-induced autophagy in the *Drosophila* fat body. Dev Cell 7:167–178

Shelly S, Lukinova N, Bambina S, Berman A, Cherry S (2009) Autophagy is an essential component of *Drosophila* immunity against vesicular stomatitis virus. Immunity 30:588–598

Sobotník J, Weyda F, Hanus R, Cvacka J, Nebesárová J (2006) Fat body of *Prorhinotermes simplex* (Isoptera: Rhinotermitidae): ultrastructure, inter-caste differences and lipid composition. Micron 37:648–656

Srivastava JP, Saxena SC (1967) On the alkaline and acid phosphatase in the alimentary tract of *Periplaneta americana* L. (*Blattaria: Blattidae*). Appl Entomol Zool 2:85–92

Terra WR, Ferreira C, de Bianchi SG (1979) Distribution of digestive enzymes among the endo- and ectoperitrophic spaces and midgut cells of *Rhynchosciara* and its physiological significance. J Insect Physiol 25:487–494

Tsukada M, Ohsumi Y (1993) Isolation and characterization of autophagy-defective mutants of *Saccharomyces cerevisiae*. FEBS 333:169–174

Umemiya-Shirafuji R, Matsuo T, Liao M, Boldbaatar D, Battur B, Suzuki H, Fujisaki K (2010) Increased expression of ATG genes during nonfeeding periods in the tick *Haemaphysalis longicornis*. Autophagy 6:473–481

Weibel ER (1979) Stereological methods, vol 1. Practical methods for biological morophometry. Academic Press, London

Weibel ER (1980) Stereological methods, vol 2. Theoretical foundations. Academic Press, London

Welinder C, Ekblad L (2011) Coomassie staining as loading control in Western blot analysis. J Proteome Res 10:1416–1419

Willott E, Bew LK, Nagle RB, Wells MA (1988) Sequential structural changes in the fat body of the tobacco hornworm, *Manduca sexta*, during the fifth larval stadium. Tissue Cell 20:635–643

Yi SX, Adams TS (2001) Age- and diapause-related acid and alkaline phosphatase activities in the intestine and Malpighian tubules of the Colorado potato beetle, *Leptinotarsa decemlineata* (Say). Arch Insect Biochem Physiol 46:152–163